

Surface ciliation and tail structure in direct-developing frog embryos: a comparison between *Myobatrachus gouldii* and *Pristimantis* (= *Eleutherodactylus*) *urichi*

Mohsen Nokhbatolfoghahai¹, Nicola J. Mitchell² & J. Roger Downie³

¹Biology Department, Faculty of Sciences, University of Shiraz, Iran

²School of Animal Biology, University of Western Australia, Australia

³Division of Ecology and Evolutionary Biology, Faculty of Biomedical and Life Sciences, University of Glasgow, UK

Surface ciliation in two direct-developing anurans from unrelated lineages, the Australian myobatrachid *Myobatrachus gouldii* and the South American terraranan *Pristimantis urichi*, is shown to be broadly similar, persisting on some body regions until close to hatching, suggesting a common need for circulation of fluid inside the jelly layers. The tail of *M. gouldii* is tadpole-like at its maximum extent though considerably reduced in its axial core and musculature. Its surface epidermis is thin and highly folded in some areas, with blood vessels approaching very close to the surface, consistent with a respiratory role. The tail moves actively when well developed, which may assist with respiratory exchange. The tail in *P. urichi* has a novel construction, quite different from both *M. gouldii* and that reported for Caribbean lineage terraranans such as *Eleutherodactylus coqui* or *E. nubicola*. In *P. urichi*, the tail expands laterally and posteriorly, not dorsally and ventrally, and only has a short axial core at its base, suggesting very limited motility: it therefore seems not to be composed of axial core and dorsal/ventral fins. We suggest that this thin-walled vascular structure, applied close to the perivitelline membrane, facilitates respiratory exchange. Discovery of this novel structure suggests that the development of other terraranan embryos needs investigation.

Key words: amphibians, ciliated cells, direct development, Myobatrachidae, Terrarana

INTRODUCTION

Direct development (endotrophy), where the embryo develops into a froglet without the usual tadpole stage, has been reported from nine families of anurans, in each case independently evolved (Thibaudeau & Altig, 1999). The details of development have so far been described in rather few species, and this is particularly the case for embryonic adaptations, i.e. those transient features that aid the development of the embryo. The most complete accounts have been provided for the direct-developing embryos of several species of Caribbean *Eleutherodactylus* (Callery & Elinson, 2000; Callery et al., 2001; Lynn, 1942; Townsend & Stewart, 1985) and three species of direct-developing myobatrachids from Australia (Anstis et al., 2007; Anstis, 2008), where some typical larval-specific features are absent (e.g. adhesive glands, teeth, jaws and lateral line) and others greatly reduced or modified (external gills, operculum, tail). Since it is common for direct development to occur in species that lay small clutches of large eggs, incubated in moist conditions on land, we might expect rather similar changes to evolve in each of the lineages of direct-developing anurans.

A particular challenge for direct-developing anuran embryos is respiratory gas exchange. The eggs of direct-developers are usually large: for example, Anstis et al.

(2007) report that the Australian *Myobatrachus gouldii* (Anura, Myobatrachidae) has ova of 5.1 mm in diameter and egg capsules 7.4 mm in diameter. A large ovum implies a relatively small surface area for respiratory exchange, and in general, larger anuran eggs have thinner jelly capsule layers that promote diffusion of respiratory gases in and out of the perivitelline space (Seymour, 1994). Moreover, direct developing species, by definition, hatch when metamorphosis is complete and hence when their rate of oxygen consumption ($\dot{V}O_2$) is at or near a peak (Mitchell & Seymour, 2000). There are generally compensatory changes in capsule morphology (the capsule becomes larger and thinner) that facilitate respiratory gas exchange at terminal embryonic stages (Seymour, 1999), but the role played by specific morphological adaptations of the anuran embryo *bauplan* is unknown.

In anuran species where there is a tadpole, but hatching is at an advanced stage, external gills tend to be particularly well developed, presumably to cope with respiratory needs (Nokhbatolfoghahai & Downie, 2008). However, in direct-developing species, external gills are usually reduced or absent (Duellman & Trueb, 1986) except in the egg-brooding hylids, which develop extensive “bell gills” (Del Pino & Escobar, 1981). A potential alternative respiratory exchange surface for direct-developing embryos is the tail (Thibaudeau & Altig, 1999; Townsend & Stewart, 1985). Its persistence when other larval fea-

tures have been deleted or reduced in most direct-developers suggests an alternative function. In *Eleutherodactylus*, the tail fins become extended and have a thin skin, long suggested to have a role in respiration (Lynn, 1942). In myobatrachids, tail development is quite variable: a respiratory role is likely in *M. gouldii* where the tail develops early, is long and has a broad, rounded, well-vascularized tip (Anstis et al., 2007).

In addition to increasing respiratory exchange surfaces, anuran embryos can improve respiration by ventilating these surfaces. Ventilation is the most obvious adaptive explanation for the complex patterns of ciliated cells found on anuran surfaces during developmental stages: embryos, early post-hatching stages and sometimes persisting until late larval stages (Nokhbatolfoghahai et al., 2005, 2006).

So far, the direct-developing embryos of myobatrachids have been examined only using low resolution light microscopy. Here, we report on scanning and transmission electron microscopic observations of the surface of *Myobatrachus gouldii* embryos, primarily aimed at elucidating respiratory adaptations, and also on direct observations of tail movements in this species.

Further, we describe new aspects of embryonic development in *Pristimantis* (= *Eleutherodactylus*) *urichi* (Anura, Terrarana), a direct-developing frog endemic to Trinidad and Tobago (Kaiser et al., 1994). Some observations on *P. urichi*, made before its taxonomic status was revised (Heinicke et al., 2007; Hedges et al., 2008), have been reported by Nokhbatolfoghahai et al. (2005). Here we make a comparison between *M. gouldii*, *Eleutherodactylus* and *Pristimantis*.

MATERIALS AND METHODS

Study species and egg collection

Myobatrachus gouldii. Anstis et al. (2007) and Anstis (2008) have reported on development in three Australian direct-developing myobatrachids: the sandhill frog (*Arenophryne rotunda*), the turtle frog (*Myobatrachus gouldii*) and Nichol's toadlet (*Metacrinia nichollsi*). The embryos of two of these species (*A. rotunda* and *M. gouldii*) develop underground at depths up to 1.5 m (Roberts, 1981, 1984), and there are small differences between species (for example, in the extent of tail development). However, all direct-developing myobatrachids show clear differences from development in *Eleutherodactylus*: the myobatrachids have no egg tooth; forelimb development is initially hidden by a reduced operculum, rather than essentially open, as in *Eleutherodactylus*; and external gills are absent, though this is a variable feature in *Eleutherodactylus*: reduced external gills have been described in some *Eleutherodactylus* but not in others (Townsend & Stewart, 1985).

Eggs of *M. gouldii* were collected from a large population in *Banksia* woodland in Pinjar State Forest, Western Australia. Until recently, eggs and embryos of this species have only been found by excavating 1–2 m below sites where males had been observed to attract a female on the soil surface (Roberts, 1981). The embryos used in

the current study were collected from matings that occurred within an enclosure constructed at the breeding site. In brief, hinged PVC pipes (1.2 m long × 15 cm diameter) buried flush to the ground were contained within a galvanized iron enclosure (about 1 m diameter) and gaps between the pipes were plugged with plaster of Paris. Courting pairs of *M. gouldii* were introduced into the enclosure in December 2007, and eggs and early-stage embryos were retrieved from the pipes between 12 and 14 February 2008.

Pristimantis urichi. Until recently, most neotropical direct-developing frogs (over 800 species) were assigned to a single genus, *Eleutherodactylus*. Heinicke et al. (2007) and Hedges et al. (2008) have used molecular phylogenetic methods to separate this large species assemblage, now named the Terrarana, into three main radiations, clades based on South America, Middle America and the Caribbean, with the Caribbean clade separating from the mainland lineage 47 million years ago. So far, comparative embryology of this group has been studied in Caribbean species, mainly *Eleutherodactylus coqui* and other Puerto Rican species (Townsend & Stewart, 1985) and the Jamaican *Eleutherodactylus* (= *Euhyas*) *nubicola* (Lynn, 1942; Frost, 2009). The long period of time separating the three clades suggests that divergences in early development could have occurred. Many of the terraranans of the South American clade, including the endemic species in Trinidad, have been assigned to the genus *Pristimantis*. *Pristimantis urichi* may be the most widely occurring frog in Trinidad (Kenny, 1969). Mainly ground-living in forested areas, these frogs have adhesive toepads and are capable of climbing some distance, with egg clutches reported at up to 2 m above ground (Murphy, 1997).

Eggs of *Pristimantis urichi* were collected from the Northern Range forests of Trinidad, West Indies in May–July 1982, 1996 and 2006. *P. urichi* is a common species throughout the Northern Range (Kenny, 1969), but finding clutches of eggs is a matter of luck. JRD has collected five batches of eggs over a period of 25 years. They have been found on damp ground under rotting wood, or amongst the leaves of decaying bromeliad plants, or in fallen humming-bird nests.

Egg incubation and fixation

Myobatrachus gouldii. Embryos were allowed to develop at room temperature (approximately 22 °C) in sand filled beakers covered in cling film, which were held within a closed styrofoam container to keep embryos in the dark.

Sixteen embryos representing a range of developmental stages were euthanased in buffered MS222, fixed in 2.5% glutaraldehyde (0.6% saline, 0.1 M phosphate buffer) and stored at 4 °C, before being sent to the University of Glasgow, under permit from the Australian Government Department of Environment, Water, Heritage and the Arts (licence No. WT2008-2588). After we had peeled off the outer jelly capsules, embryos were staged using Townsend & Stewart's (1985) table for *Eleutherodactylus*, also used by Anstis et al. (2007). Townsend & Stewart divided the pre-hatching period into 15 stages. Limb buds and tail bud appear at stages 4–

5. Digits appear on limb buds by stages 8–9. The tail is at full length with fins maximally extended by stage 10, but regresses to a stump by hatching. Embryos examined were Townsend & Stewart (TS) stages 3(2), 4(2), 5(1), 6(2), 7(2), 8(1), 9(1), 10(1) and 13(1).

Pristimantis urichi. Eggs were returned to the laboratory (University of the West Indies, or Simla Field Station) and incubated at ambient temperature (25–28 °C) on moistened tissue paper in 90 mm diameter petri dishes. Eggs were examined daily and individuals fixed at representative TS stages in Bouin's fluid or 2–5% glutaraldehyde in phosphate buffer for about 5 h, then stored in phosphate buffer at 5 °C until required for further processing. As a comparison for tail structure, swimming (exotrophic) tadpoles of *Dendropsophus* (= *Hyla*) *microcephalus* (Frost, 2009), identified using the key in Kenny (1969), were collected from field sites in Trinidad, West Indies, euthanased in MS 222 then fixed in glutaraldehyde, as for *P. urichi*.

SEM preparation and examination

Specimens were postfixed in 1% osmium tetroxide, stained in 0.5% uranyl acetate, dehydrated using an acetone series then critical-point dried, and coated with gold using a Polaron SC 515. The specimens were then examined using a JSEM 6400 scanning electron microscope over a magnification range of $\times 24$ to $\times 3200$. Images were recorded using Imageslave for Windows. At the earlier stages much of the yolky material on the ventral side of the embryo was removed prior to dehydration, because of previous experience that yolky material tends to burst open at the critical-point drying stage. Dehydration took about 30 min longer at each stage for intact specimens compared to those with yolk removed.

TEM and LM semithin section preparation and examination

Tails of *M. gouldii* were removed from embryos at Townsend & Stewart (TS) stages 6, 7 and 13 and cut into two pieces, tip and base. They were then postfixed in 1% osmium tetroxide, stained in 0.5% aqueous uranyl acetate, dehydrated using an ethanol series, then embedded in LR white resin (London Resin Company). For light microscopy (LM), semi-thin sections (0.5–1.0 μm) were stained using 1% toluidine blue in 1% borax. Sections were examined with a Leitz microscope over a range of magnifications and images were edited using Adobe Photoshop V.7 software. For transmission electron microscopy (TEM), ultrathin sections (60–70 nm) were cut then stained in 0.5% aqueous uranyl acetate, followed by lead citrate (Reynolds, 1963). Sections were washed in 0.2 N sodium hydroxide (Griffin, 1972) then examined using a LEO 912 energy filtering TEM over a magnification range of $\times 3,000$ to $\times 20,000$. Tails of *P. urichi* and *D. microcephalus* were processed in the same manner as for *M. gouldii*.

Wax histology

In order to assess the overall anatomy of the tail in *P. urichi* embryos, two TS stage 10 embryos were processed for paraffin wax histology, serially sectioned (transversely) at 7 μm and stained using haemalum and eosin.

RESULTS

Clutch size, incubation time, egg size

Myobatrachus gouldii. Clutch sizes were 5–13 eggs; development time to hatching was about 80 days at 22 °C.

Pristimantis urichi. The number of eggs found in a clutch ranged from 6 to 12. Only one clutch (12 eggs) was found at an early stage of development, so lower numbers in the others may have been the result of infection or predation. In the laboratory, eggs were prone to fungal attack, with three clutches failing after a few days. Ova near the start of incubation were 3.6 ± 0.1 mm ($n=10$) in diameter and surrounded by a thick dense jelly coat, with the overall diameter of the egg being 4.9 mm. The eggs were not adhesive to one another. We do not know the precise incubation time, but our most successful clutch was at TS stage 4, two days after collection and reached stage 6, nine days later, stage 9 after a further four days and hatched 26 days after collection following incubation at 25 °C. Townsend & Stewart (1985) estimate four days to reach stage 4, so *P. urichi* takes about 28 days to hatch, a little longer than *E. coqui* (17–26 days depending on temperature).

Myobatrachus gouldii morphology: scanning electron microscopy

General morphology. Embryos were examined at TS stages 4, 5, 6, 7, 8, 9, 10 and 13. Morphological features are shown in Figure 1. We can confirm that there are no external gills or adhesive glands, nor does the operculum have a spiracle. Forelimbs were covered by the operculum until they erupted at about stage 10. During stage 6, two conical structures were seen extending from the upper mouth margin ventrally; these became more distinct by stage 7, but reduced at stages 9, 10 and disappeared by stage 13 (Fig. 1A, B). Nostrils were small, oval and rimmed, with a distinct lacrimal groove extending from each nostril to the corresponding eye. The tail was elongated, becoming longer with time until it extended around the yolk mass as far as the head by about stage 9 (Fig. 1C). The dorsal and ventral fins were not particularly extensive, but lay flat on the yolk mass surface. The exposed tail surface showed quite extensive surface folding at the junction of fin and “axial core” (Fig. 1D). We use the term “axial core” here to denote the notochord, spinal cord and associated skeletal muscle that form the central axis of the tail.

Surface ciliation pattern. Ciliated cell density, based on the ratio of ciliated cell area to non-ciliated epidermal surface cell area, was classed into three categories (high density, $>2:1$; medium, $2:1$ to $1:1$; low, $<1:1$). Table 1 shows ciliated cell density on different body regions at different developmental stages. Ciliated cell density was low or absent on limbs and around nostrils; on other body regions, ciliated cell density increased after stages 4–5, then generally declined by the latest stage examined (stage 13) except on the ventral head, yolk sac and tail. Figure 1A, B shows the progressive reduction of ciliation on the head. Figure 1D, E, F shows persistence of tail ciliation until later stages. Figure 1G shows high density ciliation on the surface of the yolk sac at stage 7; Figure

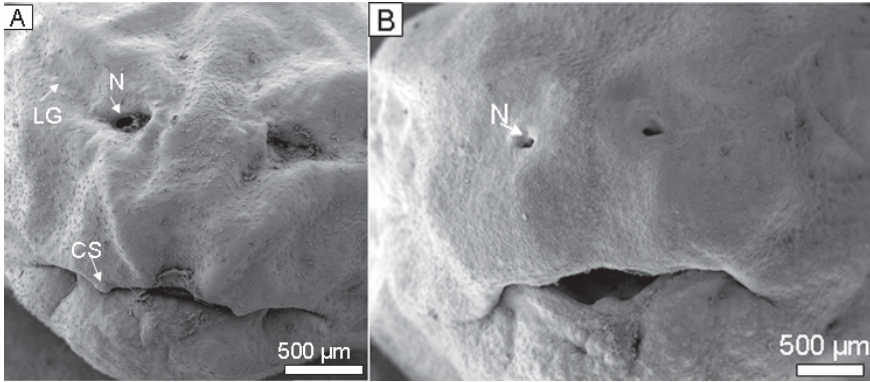


Fig. 1A, B. Head of *Myobatrachus gouldii*. A: stage 7, B: stage 10. Scanning electron micrographs showing development of conical structures (CS) on upper mouth margins and reduction of ciliation between stages 7 and 10: in these low power views, ciliated cells are small highlighted dots in 1A: absent in 1B. N, nostril; LG, lacrimal groove.

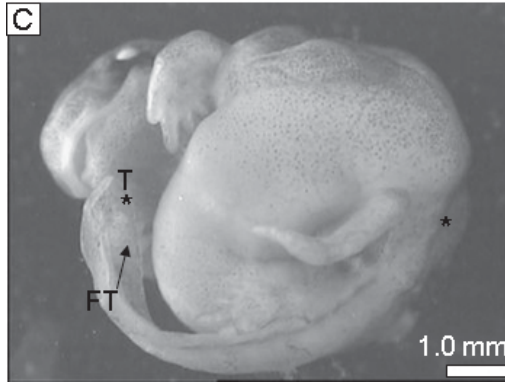


Fig. 1C. Whole embryo of *Myobatrachus gouldii*, stage 9, ventral aspect, showing elongation of tail towards head. Photomicrograph. *, base of tail; *T, tip of tail; FT, tail fin.

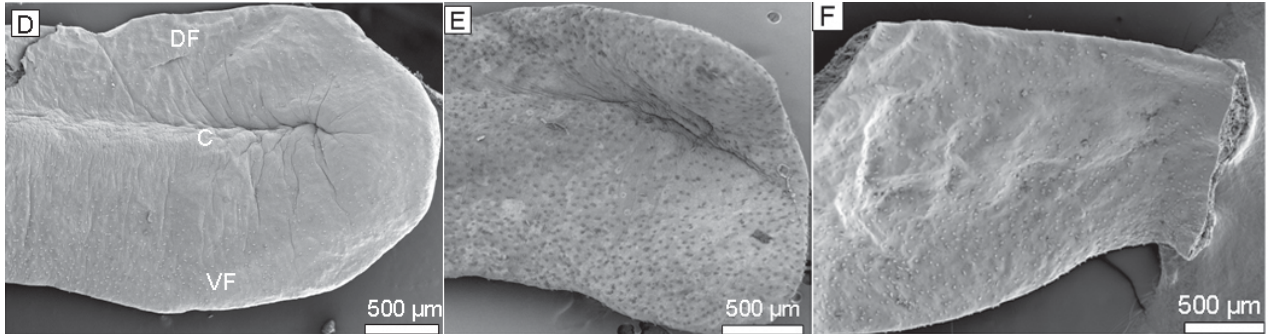


Fig. 1D, E, F. Tail of *Myobatrachus gouldii*. D: stage 7, E: stage 8, F: stage 13, showing surface ciliation and irregular folds of epidermal surface. In these lower power views, ciliated cells are small bright or dark dots scattered over the tail surface at all stages. Scanning electron micrographs. C, axial core; DF, dorsal fin; VF, ventral fin.

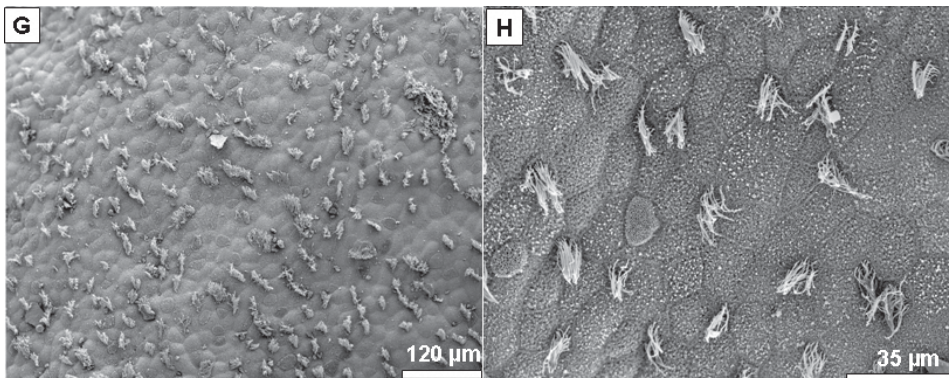


Fig. 1G, H. Higher resolution scanning electron micrographs of *Myobatrachus gouldii* surface ciliated cells. G: yolk sac at stage 7, high density ciliation. H: tail at stage 9, ciliated and pavement cells showing microvilli/microridges.

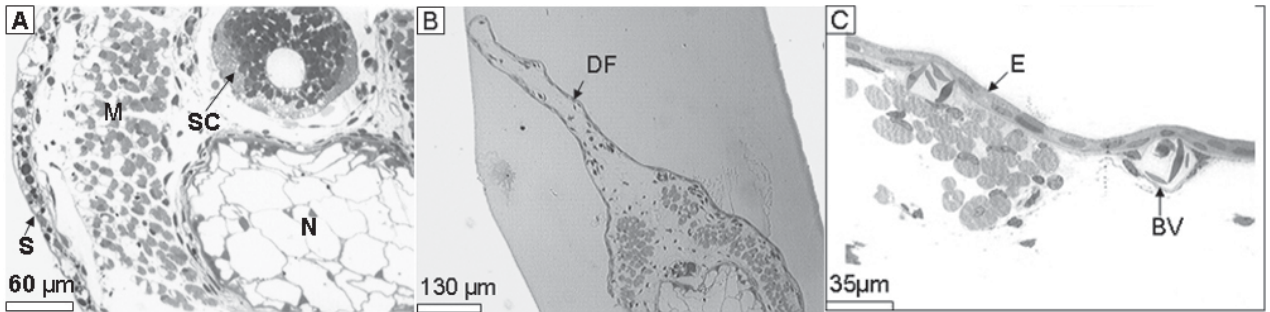


Fig. 2 A, B, C. A: Tail of *Myobatrachus gouldii* stage 6, semithin sections, stained toluidine blue. A: axial core of tail showing spinal cord (SC), notochord (N), muscle (M) and thin overlying skin (S). B: dorsal fin (DF) showing thin covering skin and relatively structureless connective tissue core, with blood vessels mainly close to skin. C: higher resolution view of fin skin with blood vessels (BV) approaching close to epidermal surface (E).

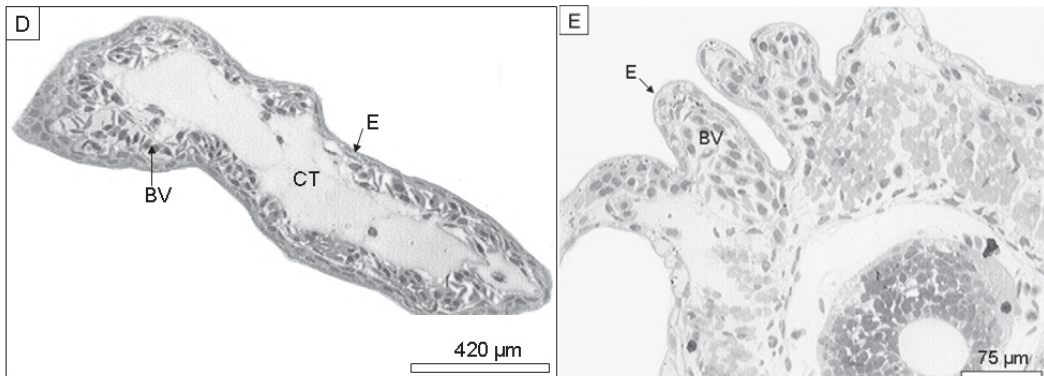


Fig. 2D, E. D: Tail tip of *Myobatrachus gouldii* stage 13, semithin section, stained toluidine blue. The tip lacks the axial core and shows abundant blood vessels (BV) embedded in loose connective tissue (CT), with a thin covering epidermis (E). E: Dorsal surface of *Myobatrachus gouldii* tail stage 7, showing surface folding. Semithin section, stained toluidine blue. The folds are irregular in shape and contain abundant blood vessels (BV) close to the epidermal surface (E).

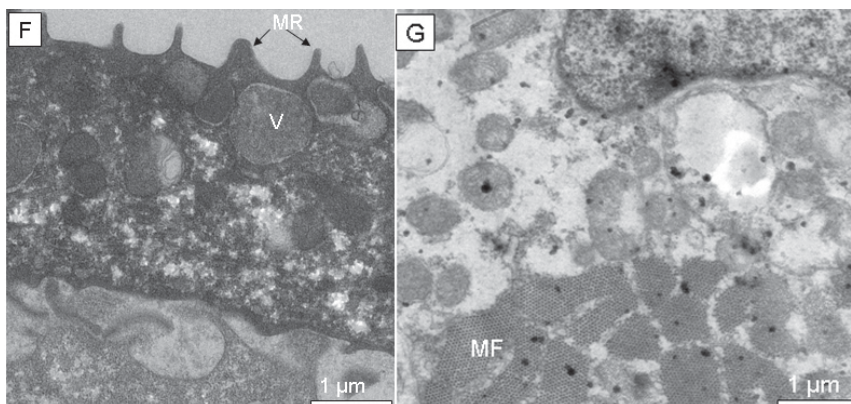


Fig. 2F, G. F: Tail surface cells of *Myobatrachus gouldii* stage 7. Transmission electron micrograph showing microridges/microvilli (MR) at outer surface, and mucus secretory vacuoles (V) in cytoplasm close to the surface. G: Muscle in tail of *Myobatrachus gouldii* stage 7. Transmission electron micrograph showing myofilament structure in cross-section (MF) typical of skeletal muscle.

1H gives a higher resolution view of ciliated and non-ciliated cells (tail, stage 9).

Semithin sections and transmission electron microscopy

Figure 2 shows that the tail has essentially normal composition with an axial core composed of dorsal spinal cord,

central notochord and lateral blocks of muscle. However, the muscle blocks are reduced compared with those in the tail of an actively swimming tadpole, such as *D. microcephalus* (Fig. 3), as is the notochord (Fig. 2A). The dorsal and ventral fins have a core of connective tissue. The overlying epidermis is thin. At higher resolution, it can be seen that the fin epidermis is underlain by blood

Table 1. Distribution of ciliated surface cells by body region and TS stage in *M. gouldii*.

| Body region | Stage | | | | | | | |
|-------------------------|-------|----|-----|-------|-----|-----|-----|-------|
| | 4 | 5 | 6 | 7 | 8 | 9 | 10 | 13 |
| Head – dorsal anterior | * | * | ** | **/** | ** | ** | ** | * |
| Head – dorsal posterior | * | * | * | * | * | * | * | 0 |
| Head – lateral | a | * | *** | *** | *** | *** | ** | n |
| Head – ventral | a | a | *** | *** | *** | *** | *** | **/** |
| Trunk – dorsal | * | * | * | * | * | * | n | n |
| Yolk sac | * | ** | ** | *** | *** | ** | *** | ** |
| Tail – stem/fins | a | a | * | ** | ** | ** | ** | ** |
| Tail – tip | a | a | */0 | * | ** | ** | ** | ** |
| Forelimbs | a | a | a | a | a | a | 0 | 0 |
| Hindlimbs | a | a | 0 | 0 | 0 | 0 | 0 | 0 |
| Nostril | a | a | 0/* | 0/* | 0/* | 0 | 0 | 0 |

0 – no ciliated cells; * – low density; ** – medium density; *** – high density; n – not available; a – structure absent.

vessels which can approach very close to the skin surface via indentations in the epidermal layer (Fig. 2B, C). The tip of the fin is rounded, rather than tapered. The basal lamina at the base of the epidermis is particularly thin at the indentations and there is a thin basal lamella. The fins extend a short distance beyond the axial core of the tail at the posterior tip, and are highly vascularized (Fig. 2D).

In sections, the surface folding seen in SEM appears as extensive folds containing prominent blood vessels close to the skin surface (Fig. 2E). The surface epidermal cells of the tail show the microvilli/microridges and mucus secretory granules typical for tadpole epidermis (Nokhbatolfoghahai & Downie, 2008) (Fig. 2F).

In section, the tail muscle is well differentiated, showing actin/myosin microfilaments in well organized patterns, characteristic of skeletal muscle, but reduced in extent compared to swimming tadpoles (Fig. 2G; Fig. 3).

Ontogenic changes in embryo movements

Embryos became capable of movement at TS stage 5, and TS stage 6 embryos moved in jerks that caused brief rotation of the trunk and tail, interspersed with bouts of vigorous tail beating lasting more than 10 s (see video 1 in online supplementary material). At TS stage 10, when the tail is at its maximum length (Anstis et al., 2007), embryos periodically waved their tails, often accompanied by twitching of the body and gentle limb movements (see video 2 in online supplementary material). Tail movement was less obvious at later developmental stages (TS stages 13–14), at which point the tail is being reabsorbed (Anstis et al., 2007). Older embryos (TS stages 14–15) were observed opening and closing the mouth, and characteristically stretched hind and forelimbs simultaneously, pushing against the perivitelline membrane. However, given that *M. gouldii* embryos would normally develop in the dark, it is unclear to what extent the movements observed reflect typical behaviours, as movements may have occurred in response to light.

Pristimantis urichi tail morphology

The distribution of ciliated cells on the surface of *P. urichi* embryos has already been described (Nokhbatolfoghahai et al., 2005). Here we provide a description of tail development and organization in *P. urichi*, which is quite different to both *M. gouldii* and *E. coqui*.

At TS stage 4, the tail bud, rather than being elongated, is essentially flat and circular, protruding posteriorly to the two hindlimb buds (Fig. 4A). The tail bud develops into a thin-walled structure that extends laterally and posteriorly, surrounding the posterior of the yolk mass and covering the hind limbs: by stage 9/10, the posteriorwards extension of the tail is maximal, reaching almost as far as the head (Fig. 4B, C, D). Thereafter, the tail regresses and near hatching is a rounded stump (Fig. 4E).

The highly vascular nature of this expanded tail is visible in whole specimens, due to the transparent thinness of the covering tissue. However, the novel organization of the tail only becomes clear in sections (Fig. 5). The extension of the tail is not due to the growth of dorsal or ventral fins, as in *M. gouldii* and *E. coqui*. Rather, the lateral body wall extends around the surface of the yolk mass, and the posterior tip of the tail also extends ventrally around the yolk mass (Fig. 5A, B). We established this arrangement through careful checking of serial sections of two embryos. In *M. gouldii* and *E. coqui*, the axial core of the tail extends along most of its length, but in *P. urichi*, the axial core is short and reduced, especially the notochord which has an unusually thin outer sheath (Fig. 5D). Most of the expanded tail lacks skeletal tissue – notochord, skeletal muscle and even neural tube (Fig. 5C): it is composed solely of thin dorsal and thinner ventral skin separating a layer of connective tissue that appears lacking in structural elements other than blood vessels. Capillaries close to the skin are more prominent on the dorsal than the ventral surface (Fig. 5D, E).

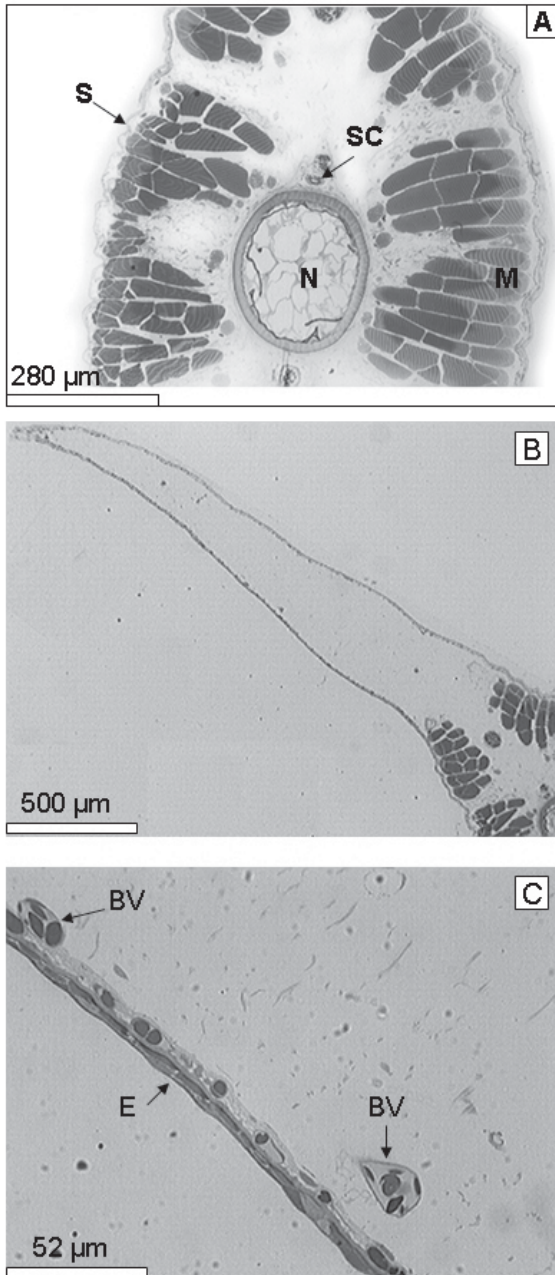


Fig. 3. Tail of a well developed *Dendropsophus* (=Hyla) *microcephalus* tadpole: semithin toluidine blue stained sections. A: axial core of tail, showing muscle blocks (M), spinal cord (SC), notochord composed of vacuolated central cells and surrounding acellular sheath (N), and overlying skin (S). B: dorsal tail fin showing loose, vascular connective tissue of the interior and overlying skin. C: higher resolution view of dorsal fin skin with blood vessels (BV) close to the surface, but not invaginated into the epidermal layer (E).

DISCUSSION

We report here on two embryonic features (surface ciliation; tail structure and motility) in direct-developing anurans from distinct lineages: *Myobatrachus gouldii*, Myobatrachidae, and *Pristimantis urichi*, South American lineage of the Terrarana.

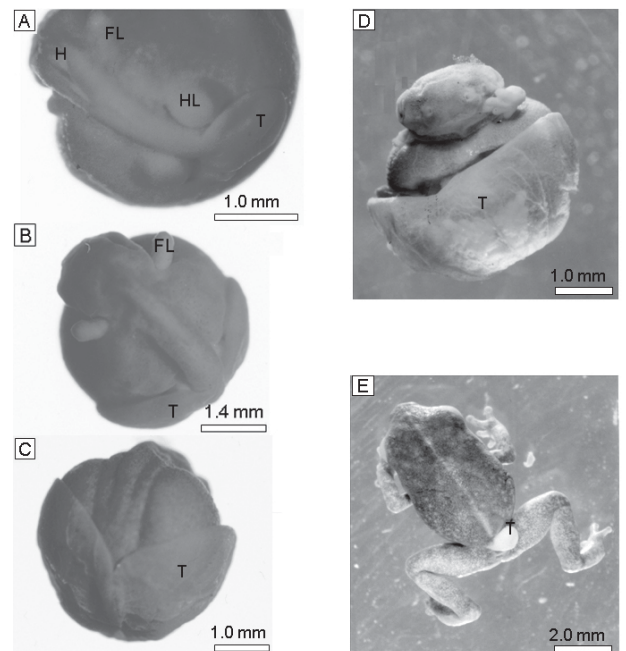


Fig. 4. Photomicrographs of complete Bouin fixed *Pristimantis urichi* embryos. Jelly capsules removed. A: TS stage 4, showing flat rounded tail bud. B, C: stage 6/7 from dorsal (B) and posterior (C) aspects to show shape and extent of expanded tail. D: stage 9/10 from ventral aspect, showing the anteriorwards extension of the tail close to the head, and the hindlimbs enclosed by the tail. E: TS stage 15, just hatched with tail a small stump only. H, head; FL, forelimb; HL, hindlimbs; T, tail.

Nokhbatolfoghahai et al. (2005) have previously reported on surface ciliation in *P. urichi* (their Table 7). Comparison with *M. gouldii* surface ciliation (this paper, Table 1) shows overall similarity: most regions of the embryonic surface in both species are extensively ciliated until relatively late stages. There are fine-scale differences: *M. gouldii* may be a little more densely ciliated overall; *P. urichi* has ciliated cells on the limb-buds at early stages, but *M. gouldii* lacks these. However, the overall picture is similar, suggesting that surface ciliation is important to embryonic development in both of these unrelated direct-developing species. It is worth noting that, at hatching, direct-developing anuran embryos are equivalent in stage to conventional anurans at the completion of metamorphosis. In most anurans, ciliated cells are most prominent in the stages around hatching, and decline as tadpoles become active swimmers, except in a few species where ciliated cells persist until later stages, especially on the tail (Nokhbatolfoghahai et al., 2005, 2006). Persistence of ciliated cells over much of the embryonic surface in both *M. gouldii* and *P. urichi* can therefore be regarded as a heterochronic change, associated with the respiratory needs of the embryo, generally regarded as the main function of surface ciliation (Nokhbatolfoghahai et al., 2005). The relative lack of cili-

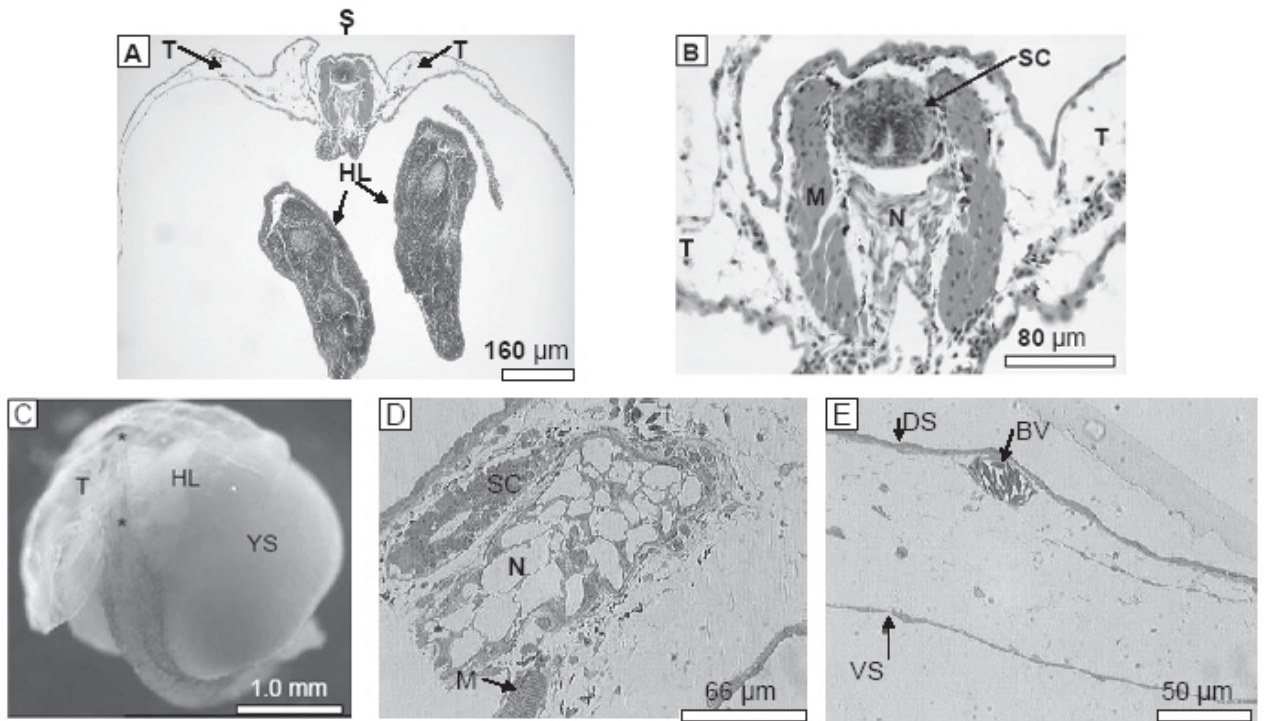


Fig. 5. Transverse sections of *P. urichi* embryo, TS stage 10 through proximal end of tail. Haemalum and eosin stained wax sections. A: Lower power view – the tail (T) extends laterally on either side of the axial core (S), not dorso-ventrally. This section is posterior to the end of the yolk sac and contains the tip of a hindlimb bud (HL). B: High power view showing the axial core with reduced spinal cord (SC), notochord (N) and skeletal muscle (M). C: Photomicrograph of complete glutaraldehyde-fixed *P. urichi*, TS stage 10 embryo, showing the short extent of the tail axial core. T, tail; HL, hindlimb; YS, yolk sac; *base and tip of tail axial core. D, E: Tails of *P. urichi*, TS stage 10 embryo. Semithin toluidine blue-stained sections. D: Axial core, showing highly reduced spinal cord (SC), notochord (N) and muscle (M). E: dorsal skin (DS) and thinner ventral skin (VS); intervening structureless connective tissue with blood vessels (BV), especially close to dorsal skin.

ated cells around the nostrils in *M. gouldii* is noteworthy: Nokhbatolfighahai et al. (2005) were unable to examine the nostril region in *P. urichi*, but in species with free-swimming tadpoles, the nostril region often possessed dense ciliation well past hatching, interpreted as a possible chemosensory role for ciliated cells. The lack of ciliated cells around the nostrils in *M. gouldii* fits with this interpretation since there is no such role prior to hatching.

An additional (and unexpected) feature of the tail in *M. gouldii* is the surface folding shown in Figure 2E. The folds are highly vascular and may therefore be an adaptation to increase respiratory exchange surface area. More embryos need to be examined to establish that this is a generally-occurring feature, but these folds do not have the appearance of a fixation artefact where tissue damage would be apparent.

Our most novel finding is that the tail in *P. urichi* is organized quite differently to that in both *M. gouldii* and in *Eleutherodactylus*. Most published figures of the *Eleutherodactylus* tail are low power drawings of the whole structure (Townsend & Stewart, 1985; Callery et al., 2001), showing that the axial core of the tail extends for

about three-quarters of the length of the tail at its maximum length, and that the vascular extensions are modified fins, positioned dorsally and ventrally, and extending caudally. The only sectional view of the *Eleutherodactylus* tail we have found (for *E. nubicola*, which remains in the genus *Euhyas* or *Eleutherodactylus*) is Figure 70 in Lynn (1942), which clearly shows, from the orientation of the neural tube and notochord, that the extensions are dorsal and ventral fins; this and his Figure 48 indicate that the tail is asymmetric, with the dorsal fin deeper than the ventral. Since the tail in *Eleutherodactylus* lies flat against the yolk sac and extends around the ventral side of the embryo towards the head, the axis of the tail must be twisted to left or right: this may be why the tail does not extend straight back, but is bent to left or right (Lynn, 1942; Townsend & Stewart, 1985). Anstis et al. (2007) show that the tail of *M. gouldii* also bends to one side, but that the fins are not as extensive as in *Eleutherodactylus*. Our sections confirm that the extensions from the axial core in *M. gouldii* are dorsal and ventral fins, of more or less equal size.

We have not found any detailed accounts of the tissue composition and state of development of the core of the

tail in *Eleutherodactylus*. In *M. gouldii*, we report that both the skeletal muscle and notochord of the tail are reduced compared to a representative swimming tadpole, and that the fin epidermis is particularly thin, with blood vessels approaching close to the surface, a feature also noticed in external gills (Nokhbatolfoghahai & Downie, 2008) and associated with respiratory exchange (Maina, 2002). Until it starts to regress, the *M. gouldii* tail is capable of vigorous movement, consistent with its structure. We expect that tail structure in *Eleutherodactylus* will be similar, given reports of its active movement (Lynn, 1942; Townsend & Stewart, 1985).

As we report, the tail in *P. urichi* is quite different. It begins as a more or less circular bud extending from the posterior end of the embryo and lying flat on the yolk-sac surface. It expands laterally and caudally around the ventral side of the yolk sac, almost reaching the head. The extensions are lateral and caudal, not dorso-ventral: they are therefore not simply modified fins. The axial core of the tail is short and highly reduced in tissue composition. Although we do not have observations of living embryos, it is highly unlikely that such a tail is more than minimally motile. Rather, it is a fixed highly vascular respiratory exchange surface covering a large proportion of the embryo's outer surface, and in close contact with the investing vitelline membrane and jelly coat. As far as we can tell, this is a novel observation, though Thibaudeau & Altig (1999) give a brief description of what may turn out to be similar structure in *Eleutherodactylus* (= *Pelorius*) *inoptatus*, a species from Hispaniola (Frost, 2009), and the "bell gills" of egg-brooding hylids may be analogous in structure and function (Del Pino & Escobar, 1981).

Until now, only embryos of the Caribbean lineage of the Terrarana (Hedges et al., 2008) have been fully investigated. We show here that at least one species of the South American lineage has a novel embryonic feature. It will be interesting to discover whether the novel tail structure found in *P. urichi* is characteristic of the lineage, how it has been derived – assuming that the simpler tail of *Eleutherodactylus* is ancestral – and whether it confers any measureable advantages in development time or metabolic rate. Whether *Pristimantis* shows other novel features requires detailed analysis of more complete developmental series than we have been able to access.

ACKNOWLEDGEMENTS

We thank Margaret Mullin and Andrew Lockhart for technical assistance with material preparation. We also thank Victoria Cartledge, Caitlin O'Neill, Amanda Worth and Karen Riley for assistance collecting *M. gouldii* eggs, students on University of Glasgow expeditions to Trinidad for finding eggs of *P. urichi* on occasion, Kathleen Rennison for preliminary observations on these embryos, and staff at the University of the West Indies for kindly providing laboratory space. *M. gouldii* embryos were collected under licence SF006086 from the Western Australian Department of Environment and Conservation. We thank camera man Greg Knight and Australian Geographic for the video footage of *M. gouldii* embryos. JRD

acknowledges financial assistance with fieldwork from the Carnegie Trust and the University of Glasgow, NJM acknowledges funding from the University of Western Australia and Australian Geographic, and MN acknowledges financial support from the University of Shiraz, Iran.

REFERENCES

- Anstis, M. (2008). Direct development in the Australian myobatrachid frog *Metacrinia nichollsi* from Western Australia. *Records of the Western Australian Museum* 24, 133–150.
- Anstis, M., Roberts, J.D. & Altig, R. (2007). Direct development in two myobatrachid frogs, *Arenophryne rotunda* Tyler and *Myobatrachus gouldii* Gray, from Western Australia. *Records of the Western Australian Museum* 23, 259–271.
- Callery, E.M. & Elinson, R.P. (2000). Thyroid hormone-dependent metamorphosis in a direct developing frog. *Proceedings of the National Academy of Sciences, USA* 97, 2615–2620.
- Callery, E.M., Fang, H. & Elinson, R.P. (2001). Frogs without polliwogs: evolution of anuran direct development. *Bioessays* 23, 233–241.
- Del Pino, E.M. & Escobar, B. (1981). Embryonic stages of *Gastrotheca riobambae* (Fowler) during maternal incubation and comparison of development with that of other egg-brooding hylid frogs. *Journal of Morphology* 167, 277–295.
- Duellman, W.E. & Trueb, L. (1986). *Biology of Amphibians*. New York: McGraw Hill.
- Frost, D.R. (2009). *Amphibian Species of the World. An Online Reference, Version 5.3* (12 February 2009). Electronic database accessible at <http://research.amnh.org/herpetology/amphibia/index.php>. New York: American Museum of Natural History.
- Gosner, K.L. (1960). A simplified table for staging anuran embryos and larvae with notes on identification. *Herpetologica* 16, 183–190.
- Griffin, R.L. (1972). *Ultramicrotomy*. London: Bailliere Tindall.
- Hedges, S.B., Duellman, W.E. & Heinicke, M.P. (2008). New World direct-developing frogs (Anura: Terrarana): molecular phylogeny, classification, biogeography, and conservation. *Zootaxa* 1737, 1–182.
- Heinicke, M.P., Duellman, W.E. & Hedges, S.B. (2007). Major Caribbean and Central American frog faunas originated by ancient oceanic dispersal. *Proceedings of the National Academy of Sciences, USA* 104, 10092–10097.
- Kaiser, H., Hardy, J.D. & Green, D.M. (1994). Taxonomic status of Caribbean and South American frogs currently ascribed to *Eleutherodactylus urichi* (Anura: Leptodactylidae). *Copeia* 1994, 780–796.
- Kenny, J.S. (1969). The amphibia of Trinidad. *Studies of the Fauna of Curaçao and Other Caribbean Islands* 29, 1–78.
- Lynn, W.G. (1942). The embryology of *Eleutherodactylus nubicola*, an anuran which has no tadpole stage. *Contributions to Embryology* 30, 27–62.

- Maina, J.N. (2002). Structure, function and evolution of the gas exchangers: comparative perspectives. *Journal of Anatomy* 201, 281–304.
- Mitchell, N.J. & Seymour, R.S. (2000). Effects of temperature on the energy cost and timing of embryonic and larval development of the terrestrially breeding moss frog, *Bryobatrachus nimbus*. *Physiological and Biochemical Zoology* 73, 829–840.
- Mitchell, N.J. & Seymour, R.S. (2003). The effects of nest temperature, nest substrate and clutch size on the oxygenation of embryos and larvae of the Australian moss frog, *Bryobatrachus nimbus*. *Physiological and Biochemical Zoology* 76, 60–71.
- Murphy, J.C. (1997). *Amphibians and Reptiles of Trinidad and Tobago*. Florida: Krieger.
- Nokhbatolfoghahai, M. & Downie, J.R. (2008). The external gills of anuran amphibians: comparative morphology and ultrastructure. *Journal of Morphology* 269, 1197–1213.
- Nokhbatolfoghahai, M., Downie, J.R., Clelland, A.R. & Rennison, K. (2005). The surface ciliation of anuran amphibian embryos and early larvae: patterns, timing differences and functions. *Journal of Natural History* 39, 887–929.
- Nokhbatolfoghahai, M., Downie, J.R. & Ogilvy, V. (2006). The surface ciliation of anuran amphibian larvae: persistence to late stages in some species but not others. *Journal of Morphology* 267, 1248–1256.
- Reynolds, E.S. (1963). The use of lead citrate at high pH as an electron opaque stain in electron microscopy. *Journal of Cell Biology* 17, 208–213.
- Roberts, J.D. (1981). Terrestrial breeding in the Australian leptodactylid frog *Myobatrachus gouldii* (Gray). *Australian Wildlife Research* 8, 451–62.
- Roberts, J.D. (1984). Terrestrial egg deposition and direct development in *Arenophryne rotunda* Tyler, a myobatrachid frog from coastal sand dunes at Shark Bay, W.A. *Australian Wildlife Research* 11, 191–200.
- Seymour, R.S. (1994). Oxygen diffusion through the jelly capsules of amphibian eggs. *Israel Journal of Zoology* 40, 493–506.
- Seymour, R.S. (1999). Respiration of aquatic and terrestrial amphibian embryos. *American Zoologist* 39, 261–270.
- Thibaudeau, G. & Altig, R. (1999). Endotrophic anurans: development and evolution. In *Tadpoles: The Biology of Anuran Larvae*, 170–188. McDiarmid, R.W. & Altig, R. (eds). Chicago: University of Chicago Press.
- Townsend, D.S. & Stewart, M.M. (1985). Direct development in *Eleutherodactylus coqui* (Anura: Leptodactylidae): a staging table. *Copeia* 1985, 423–436.

Accepted: 11 January 2010